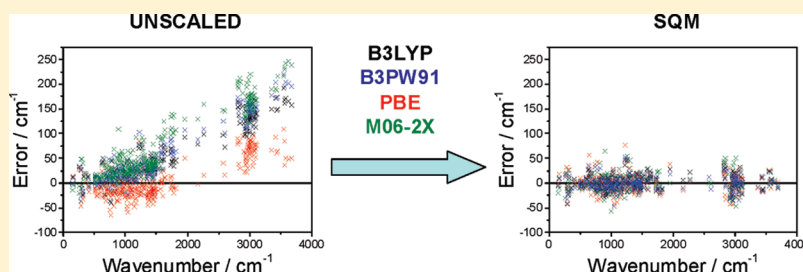# Gas-Phase and Ar-Matrix SQM Scaling Factors for Various DFT Functionals with Basis Sets Including Polarization and Diffuse Functions

Csaba Fábri, Tamás Szidarovszky, Gábor Magyarfalvi, and György Tarczay*

Laboratory of Molecular Spectroscopy, Institute of Chemistry, Eötvös University, P.O. Box 32, 1518 Budapest 112, Hungary

Ⓢ Supporting Information

ABSTRACT:

Scaling factors for Pulay's scaled quantum mechanical (SQM) scheme have been determined for four different widely used DFT functionals (PBE, B3LYP, B3PW91, and M06-2X) and for two basis sets (6-31++G** and aug-cc-pVTZ) by fitting computed results to 347 fundamental experimental vibrational frequencies of 33 molecules. Measurements in the gas phase and in solid argon matrices were used independently in the fitting procedure in order to provide a simple method of estimating matrix shifts. The accuracy of the new scaling factors is demonstrated on test molecules including hydrogen-bonded systems and molecules containing chlorine and sulfur atoms.

1. INTRODUCTION

Comparison of measured vibrational frequencies with calculated values is nowadays practically unavoidable when experimentalists interpret and assign vibrational spectra in order to identify molecular structures, conformations, or novel species. There is obviously a need for simple and reliable computational methods of estimating vibrational frequencies.

The precision of vibrational spectra calculated by quantum chemical methods has improved significantly in the last few decades. The first *ab initio* harmonic frequency calculations were done using Hartree–Fock theory and predicted vibrational frequencies with an average error of about 10% without empirical corrections.[1] Nowadays, spectra are routinely calculated using density functional theory (DFT) methods. The results, still based on the harmonic approximation, reproduce experimental values much better, with average errors usually below 4–5%.[2]

For small molecules one can go beyond the harmonic approximation, treating anharmonicities by either perturbational or variational procedures. For example, second-order vibrational perturbation (VPT2) theory[3] is implemented in many quantum chemical packages, e.g., Gaussian03,[4] PSI,[5] ACES III,[6] or CFOUR,[7] and can routinely be used for most rigid or semirigid molecules. Many VPT2 calculations utilize quartic anharmonic force fields usually calculated by high-level electronic structure methods (e.g., MP2, CCSD, or CCSD(T)) or via

DFT using medium-sized Dunning-type basis sets (e.g., (aug-)cc-pVTZ or (aug-)cc-pVQZ).[8] Except for special cases, when vibrational resonances are not properly accounted for or when the electronic structure calculations require multireference treatments, a VPT2 CCSD(T)/cc-pVQZ computation usually has an average error of only a few wavenumbers.[3b,c]

Even higher accuracy can be achieved by variational or quasi-ivariational methods for describing nuclear motion, combined with state-of-the-art *ab initio* potential energy surfaces. Using extrapolation schemes to estimate full electron correlation and complete basis set results, and including diagonal Born–Oppenheimer and relativistic corrections, an accuracy of ~1 cm^{-1} can be reached for fundamental transitions.[9] One of the main problems with these state-of-the-art calculations is their computational cost. At present, VPT2 CCSD(T)/cc-pVQZ calculations can typically be performed for systems containing not more than about 15–20 atoms. Not only the cost, but also the absence of effective programs, limits nuclear variational calculations in practice to systems containing only 3–6 atoms.

For most spectroscopic studies dealing with larger molecules, the above methods are obviously unrealistic; thus, Hartree–Fock
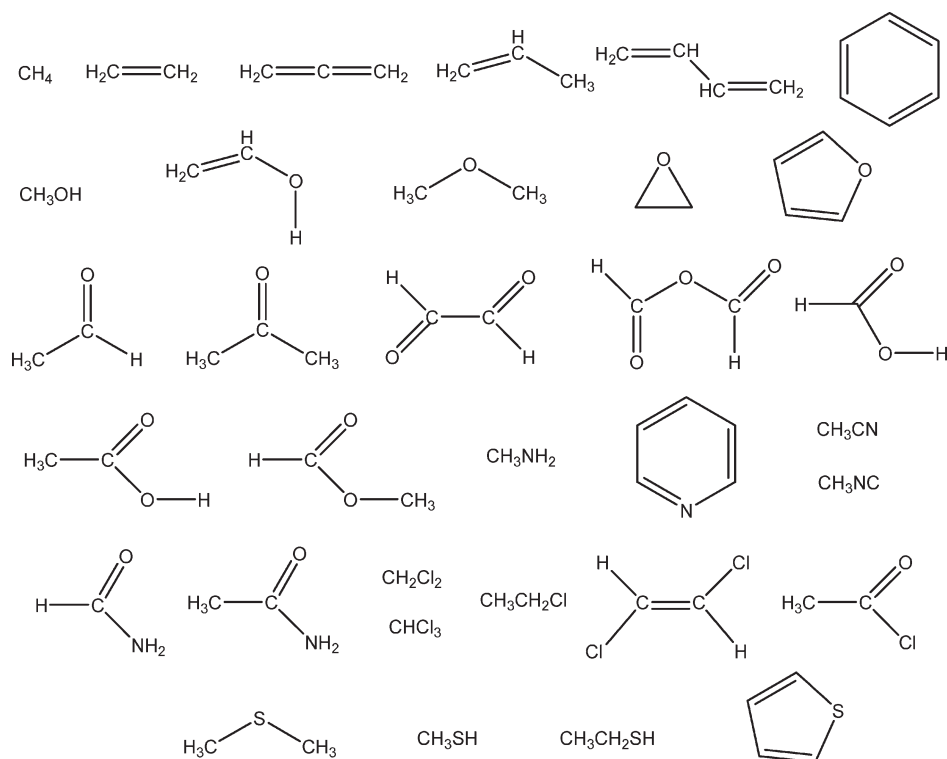
Figure 1. Molecules in the SQM training set.

or DFT theory and the harmonic approximation remain the practical compromise. Fortunately, the errors in these approximations, arising mainly from an incomplete description of electron correlation and the neglect of anharmonicity, are fairly systematic, and thus can be corrected for empirically.

A single (uniform) scaling factor for frequencies is often used to improve agreement with experimental frequencies.[10] Also, different scaling factors may be used for different regions of the IR spectra or for different normal modes.[11] Still, these schemes of scaling cannot take into account the different scaling requirements of strongly mixed vibrational modes.

This problem can be eliminated by the more sophisticated scaled quantum mechanical (SQM) empirical correction procedure.[12] This scheme employs different scaling factors for different types of *force constants* F_{ij} (rather than frequencies) expressed in internal coordinates (e.g., stretching, bending, etc.). The physical consideration behind individual scaling is that both the errors of a given electronic structure calculation and anharmonicity may be different for different distortions of the molecule. In practice, internal coordinates are grouped according to their chemical type: a factor s_i is assigned to each group, and diagonal force constants are multiplied by the relevant s_i, while the geometric mean is used for couplings:

$$F_{ij}(\text{scaled}) = (s_i s_j)^{1/2} F_{ij} \qquad (1)$$

Originally, the major drawback of the SQM scheme was the need to define and generate the internal coordinates. Although the automatic generation of "natural" internal coordinates has been solved,[13] a variant SQM scheme, suggested also by Pulay's group, seems more pragmatic. This is applied to a redundant set of primitive internal coordinates, scaling the individual stretchings, bendings, and torsions.[16]

The scheme can be easily employed, and its computational cost is negligible once the unscaled force constant matrix is available. It may be not quite obvious that SQM scaling usually improves the calculated vibrational intensities as well. This is plausible; however, we realize that the form of the normal vibrations (as a linear combination of internal coordinates) has been improved.

A minor drawback of both the single scaling factor and the SQM procedure is that in principle different scaling factors have to be determined for each level of theory, including the electronic structure method (or the functional for DFT) and, at least if one is far from the basis set limit, the basis set.[10]

The first consistent set of scaling factors was determined for HF/4-21G calculations.[12] Later on, scaling factors were optimized for DFT calculations, at BLYP/6-31G* and B3LYP/6-31G* levels.[14−16] These were limited to molecules containing H, C, N, O, and Cl atoms. The SQM method was extended to Si-containing molecules by Kalincsák and Pongor.[17] In a very recent paper scaling factors for the larger 6-311G** basis set were published.[18]

The above methods and specifically the standard SQM B3LYP/6-31G* scheme predict vibrational frequencies with an average error of about 10 cm^{-1} in most cases. However, special projects may need another DFT functional and/or basis set, necessitating the optimization of new scale factors.

The present study has several goals. The first was to determine SQM scaling factors for a level of theory which is suitable for hydrogen-bonded systems, e.g., hydrogen-bonded dimers or "biomolecule"—water complexes, model peptides or drug molecules. To accurately describe hydrogen bonding, diffuse and polarization functions are required, so we tested the Pople-type 6-31++G**[19] and the Dunning-type aug-cc-pVTZ[20] basis sets.

For selecting the DFT method, many functionals have been tested for hydrogen-bonded systems.[21,22] The frequently used

Table 1. Gas-Phase SQM Scaling Factors with Root-Mean-Square (RMS) Errors and Mean-Average Deviations (MAD) of the Fit in cm^{-1}

internal coordinate	PBE		B3LYP		B3PW91		M06-2X	
	6-31++G**	aug-cc-pVTZ	6-31++G**	aug-cc-pVTZ	6-31++G**	aug-cc-pVTZ	6-31++G**	aug-cc-pVTZ
X–X	0.9876	0.9902	0.9367	0.9471	0.9149	0.9276	0.8788	0.8910
X–{Cl,S}	1.0907	1.0959	1.0581	1.0725	0.9894	0.9973	0.9434	0.9523
C–H	0.9569	0.9676	0.9172	0.9282	0.9094	0.9235	0.8966	0.9061
N–H	0.9550	0.9655	0.9118	0.9200	0.8984	0.9089	0.8907	0.9008
O–H	0.9747	0.9825	0.9151	0.9218	0.8981	0.9073	0.8798	0.8868
S–H	0.9786	0.9840	0.9378	0.9417	0.9178	0.9264	0.8958	0.8978
X–X–X	1.0882	1.0815	1.0140	0.9992	1.0071	1.0076	0.9711	0.9547
X–X–H	1.0348	1.0397	0.9639	0.9683	0.9671	0.9762	0.9630	0.9677
H–C–H	1.0188	1.0236	0.9491	0.9573	0.9587	0.9711	0.9483	0.9545
H–N–H	1.0109	1.0354	0.9513	0.9591	0.9497	0.9667	0.9594	0.9773
X–X–X–X	1.0604	1.0251	0.9865	0.9621	0.9825	0.9723	0.9649	0.9479
{H,X}–X–X–H	1.0361	1.0204	0.9564	0.9461	0.9546	0.9433	0.9221	0.9134
(linear bend)^a	0.9144	0.9533	0.8600	0.8987	0.8567	0.9018	0.8114	0.8352
				No Scaling				
rms	37.77	34.26	70.39	61.92	78.48	67.27	93.74	85.29
MAD	19.16	15.08	39.78	34.11	45.71	39.15	52.93	47.11
				Uniform Scaling				
scaling factor^b	0.9774	0.9853	0.9289	0.9375	0.9210	0.9327	0.9058	0.9139
rms	32.30	31.72	23.28	21.45	25.34	24.49	27.23	25.02
MAD	11.19	12.38	8.46	8.77	9.39	10.26	11.47	11.36
				SQM Scaling				
rms	15.42	20.18	13.13	13.45	12.68	14.63	15.46	14.94
MAD	7.83	10.70	6.66	6.98	6.31	7.30	7.72	7.44

^{a} Only the C–C–N and C–N–C scaling factor of CH$_3$CN and CH$_3$NC is included in the fit; furthermore, it can be very different for different molecules. Hence, this value is not transferable to other molecules. ^{b} Scaling factor for force constants. The scaling factor of the vibrational frequencies is the square-root of the given value.

B3LYP[23] and PBE[24] functionals were chosen for the present study. These functionals also perform reasonably well for relative conformer energies and vibrational frequencies, which are also important for conformational studies using infrared (IR) spectroscopy. In addition, to get information on molecules where intramolecular dispersion forces are not negligible, the M06-2X functional[25] was also included in the present study.

Our second goal was to obtain a scheme specifically for vibrational circular dichroism (VCD) spectra, an increasingly popular method for determining absolute molecular conformations. To this purpose, beside the widely used B3LYP,[23] the B3PW91[26] functional proved to be successful[27] and is therefore included in the present study, using Pople-type split-valence or Dunning-type, e.g., aug-cc-pVTZ, basis sets.

A third goal of the present study is to include molecules containing sulfur in the SQM scaling factor fitting set. The inclusion of sulfur is important for studies of peptides containing methionine, cysteine, or cystine.

Another objective of the present study was to separately fit SQM scaling factors to frequencies measured in the gas-phase and in matrix isolation (in solid argon), respectively. Both experimental methods are frequently used for conformational studies. The differences in scaling factors can give information about matrix shifts for specific vibrational modes. The possible physical origins of these shifts between gas-phase and Ar matrix measurements are also discussed.

2. COMPUTATIONAL DETAILS

Electronic structure calculations have been performed with the Parallel Quantum Solutions (PQS)[28] and the Gaussian 09 program packages.[4] Calculations employed standard split-valence, 6-31++G**,[19] and correlation-consistent, aug-cc-pVTZ,[20] basis sets. Both types of basis sets contain diffuse functions, adequate for the description of hydrogen bonding. The functionals are also standard and well-documented, B3LYP,[23] PBE,[24] B3PW91[26] and M06-2X.[25] For calculations involving the first three of these PQS was used, while for the latter we used Gaussian09. Scaling factors were fitted using the SQM 1.0 module of PQS. A script was especially written to interface SQM with Gaussian 09. Throughout this study the modified SQM procedure of Baker et al. was used.[16]

Experimental vibrational frequencies measured in the gas phase and in Ar matrices were collected from the literature. Figure 1 shows the structures of the molecules included in the training set for the fitting procedure. Altogether 347 vibrations from 33 molecules were included. The total number of vibrational modes is somewhat smaller than in previous SQM fitting studies, since in the present paper only those vibrational modes were considered for which both gas-phase and Ar-matrix frequency data were available. Furthermore, vibrational modes with possible vibrational resonances and uncertain assignments were excluded from the fitting set. In each case the mass of the

Table 2. Ar-Matrix SQM Scaling Factors with Root-Mean-Square (RMS) Errors and Mean-Average Deviations (MAD) of the Fit in cm^{-1}

	PBE		B3LYP		B3PW91		M06-2X	
internal coordinate	6-31++G**	aug-cc-pVTZ	6-31++G**	aug-cc-pVTZ	6-31++G**	aug-cc-pVTZ	6-31++G**	aug-cc-pVTZ
X—X	0.9833	0.9865	0.9321	0.9424	0.9108	0.9236	0.8748	0.8865
X—{Cl,S}	1.0835	1.0905	1.0480	1.0621	0.9789	0.9893	0.9336	0.9420
C—H	0.9586	0.9693	0.9189	0.9299	0.9111	0.9251	0.8982	0.9078
N—H	0.9491	0.9595	0.9061	0.9143	0.8928	0.9033	0.8852	0.8952
O—H	0.9658	0.9735	0.9067	0.9134	0.8899	0.8990	0.8718	0.8786
S—H	0.9855	0.9910	0.9445	0.9484	0.9243	0.9330	0.9020	0.9041
X—X—X	1.0932	1.0689	1.0219	1.0083	1.0114	1.0001	0.9740	0.9600
X—X—H	1.0346	1.0400	0.9635	0.9681	0.9665	0.9762	0.9625	0.9679
H—C—H	1.0087	1.0129	0.9394	0.9479	0.9490	0.9607	0.9386	0.9447
H—N—H	0.9995	1.0234	0.9407	0.9485	0.9392	0.9556	0.9488	0.9662
X—X—X—X	1.0935	1.0617	1.0161	0.9914	1.0093	0.9930	0.9877	0.9724
{H,X}—X—X—H	1.0412	1.0272	0.9623	0.9498	0.9610	0.9531	0.9283	0.9184
(linear bend)^a	0.9720	1.0088	0.9129	0.9492	0.9095	0.9514	0.8632	0.8869
				No Scaling				
rms	37.57	33.99	70.83	62.42	78.98	67.42	94.18	85.74
MAD	19.86	15.64	39.39	33.76	45.55	38.67	52.83	47.03
				Uniform Scaling				
scaling factor^b	0.9769	0.9847	0.9284	0.9369	0.9205	0.9322	0.9053	0.9133
rms	31.73	31.42	23.04	21.33	25.30	23.54	26.96	24.80
MAD	11.14	12.16	9.08	9.24	9.79	9.92	10.79	11.01
				SQM Scaling				
rms	15.81	20.82	13.29	13.86	12.99	13.37	15.31	14.92
MAD	7.72	10.81	6.77	6.95	6.49	6.84	7.70	7.55

^{a} Only the C—C—N and C—N—C scaling factor of CH$_3$CN and CH$_3$NC is included in the fit; furthermore, it can be very different for different molecules. Hence, this value is not transferable to other molecules. ^{b} Scaling factor for force constants. The scaling factor of the vibrational frequencies is the square-root of the given value.

most abundant isotope was used in the frequency calculations. The experimental vibrational frequencies together with their references are given in the Supporting Information.

The initial set of scaling factors was practically the same as in ref 16. Only small modifications were made during the fitting procedure (see Section 3 for details) either to obtain a better fit, or to get a better model for the different matrix shifts.

3. RESULTS AND DISCUSSION

3.1. Fitting Results for Different Computational Levels. The SQM and single uniform scaling factors fitted for gas-phase and Ar-matrix experimental data at eight different levels of theory are summarized in Tables 1 and 2. In these tables, the root-mean-square (rms) errors and mean average deviations (MAD) between the computed and the experimental frequencies are also given.

Compared to ref 16, X—{Cl,S} and H—S stretching force constants were added to the original set, and X—X—X—X and the {H,X}—X—X—H scaling factors were fitted independently in the present study, because the obtained Ar-matrix scaling factors were significantly different for these force constants. (Here and elsewhere in this work, X denotes any non-H atom which is not specifically defined by another scaling factor.) Other types of scaling factors (e.g., X—X—X—H and H—X—X—H instead of

{H,X}—X—X—H) were also tested, but neither for gas-phase nor for Ar-matrix experimental values did these fits give considerably smaller rms error and MAD values than the reported sets of scaling factors.

Figures 2 and 3 show the errors in the unscaled, the uniformly scaled, and the SQM scaled computed vibrational frequencies (obtained using the 6-31++G** basis set) when compared to the gas-phase and Ar-matrix experimental vibrational frequencies. Without scaling, the PBE functional gives the smallest rms and MAD values for frequencies. This is in line with systematic benchmark studies on comparisons of DFT functionals, which showed that PBE is one of the best performing DFT functionals for harmonic vibrational frequency calculations. It is also in agreement with former studies[2,29] that M06-2X provides poorer results for unscaled vibrational frequencies. B3LYP and B3PW91 perform in between the PBE and the M06-2X functionals in this respect.

The above order does not hold for the scaled frequencies. As Figures 2 and 3 show, the individual error as a function of wavenumber is considerably less linear and thus less systematic for the PBE functional than for the other three functionals. As a consequence, both the uniformly and the SQM scaled vibrational frequencies have considerably smaller rms error and MADs for the other three functionals.

Most scaling factors increase when the basis set is changed from 6-31++G** to aug-cc-pVTZ. However, scaling factors for the
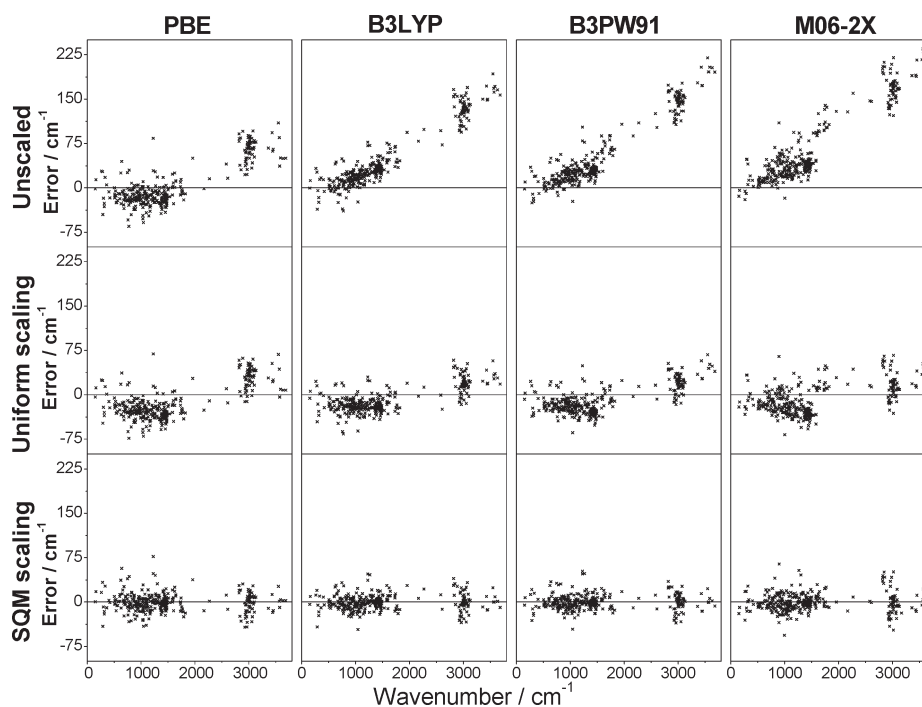
Figure 2. Errors in calculated vibrational frequencies $(\tilde{\nu}_{gas,calc} - \tilde{\nu}_{gas,\,exp}\ vs\ \tilde{\nu}_{gas\,exp})$ for the vibrational modes of the training set using different types of scaling and different DFT functionals with the 6-31++G** basis set.
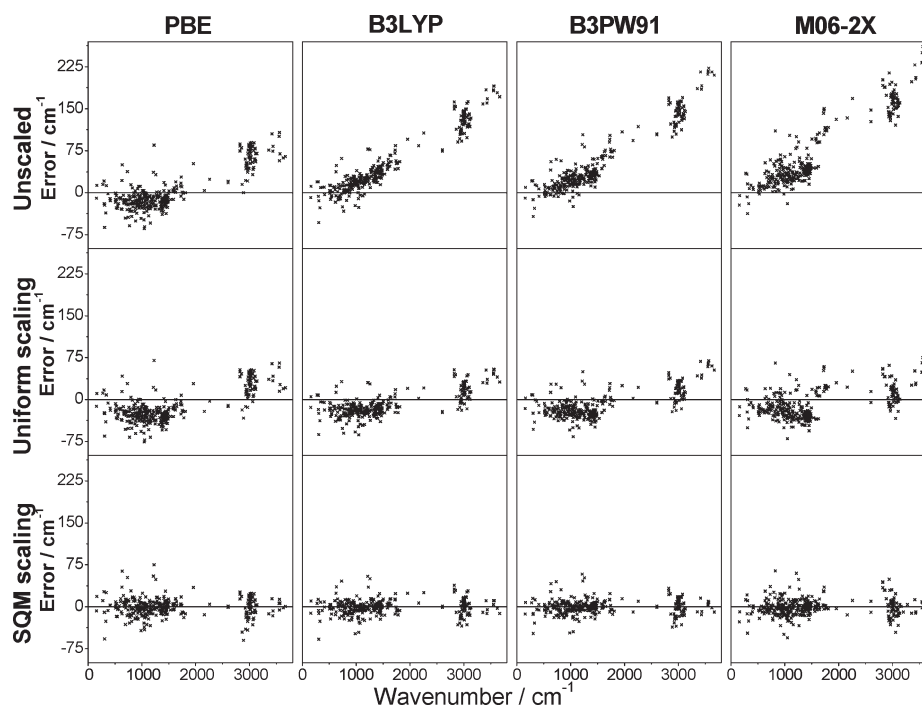
Figure 3. Errors in calculated vibrational frequencies $(\tilde{\nu}_{Ar,calc} - \tilde{\nu}_{Ar,exp}\ vs\ \tilde{\nu}_{Ar,exp})$ for the vibrational modes of the training set using different types of scaling and different DFT functionals with the 6-31++G** basis set.

X—X—X bending deformations and the torsions consistently decrease. The X—X—X—X torsional vibrations show a large decrease in the magnitude of the scaling factor with all DFT functionals, but generally the sensitivity of the SQM scaling factors to the quality of the basis set is different for different functionals. The following vibrations show a relatively larger change in the respective factor value when the basis set is changed: H—N—H vibrations for the PBE functional, X—{Cl,S} and X—X—X vibrations for B3LYP, X—X, C—H, and H—N—H vibrations for B3PW91, and X—X—X and the H—N—H vibrations for M06-2X.

Since DFT methods converge fairly rapidly with the one-particle basis set a uniform scaling factor obtained for a given

functional with a large enough basis set can be used in calculations applying a different large basis set with the same functional. In contrast to this, in the case of SQM scaling it is more important to use scaling factors optimized for the particular basis set, especially far from the complete basis set limit. This is because SQM scaling factors can change differently with different basis sets; i.e., some of them may increase, while others may decrease. This usually averages out for the uniform scaling factor. As an example, the gas-phase PBE H−N−H scaling factor increases by 0.025 and the X−X−X−X scaling factor decreases by 0.035, while the uniform scaling factor increases by only 0.008 when the basis set is changed from 6-31++G** to aug-cc-pVTZ. In order to illustrate this we used the optimized B3LYP/6-31G* (refs 10 and 16) and the gas-phase B3LYP/6-31++G** (Table 4) scaling factors to scale the B3LYP/aug-cc-pVTZ force fields of the molecules in the training set. In the case of SQM scaling the total rms error increases from 13.45 cm^{-1} to 55.53 cm^{-1} and to 16.25 cm^{-1}, respectively. In the case of uniform scaling the change in the rms errors is smaller, increasing from 21.45 cm^{-1} to 25.04 cm^{-1} and to 23.08 cm^{-1}, respectively. Interchanging the scaling factors between different functionals leads to much larger rms errors.

As seen in Tables 1 and 2 the rms error decreases by almost half, and the MAD to two-thirds, on changing from uniform scaling to the SQM scheme. (Illustrative examples when the slightly more elaborate SQM procedure has obvious benefits are shown in Section 3.3 for molecules not in the training set.) It is important to note that even the M06-2X functional, which was found to be inferior for unscaled vibrational frequency calculations, when used together with the SQM scheme gives considerably better results than any of the functionals using a single uniform scaling factor. Moreover, the M06-2X SQM vibrational frequencies have similar rms and MAD values compared to those of the other functionals with the SQM method, and at the same time are expected to be more accurate in cases when inter- and intramolecular hydrogen bonds can influence the vibrational frequencies.

Finally, it is also interesting to note that, except for the Ar-matrix SQM M06-2X frequencies, both the MAD and rms errors are smaller for the 6-31++G** basis set than for aug-cc-pVTZ. This means that the smaller 6-31++G** basis set with a DFT functional and SQM scaling can efficiently be used for the calculation of vibrational spectra of large molecules.

3.2. Comparison of SQM Scaling Factors Fitted to Gas-Phase and Ar-Matrix Frequencies. It is not obvious whether the effect of the matrix host on the vibrational frequencies can be modeled simply by using separate SQM scaling factors for gas-phase and Ar-matrix data, respectively. Of course, specific interactions cannot be treated by scaling. Notable are, for example, site splitting effects in which vibrational bands are split due to embedding of the investigated molecule into differently shaped cavities in the host lattice. These effects are expected to be specific for individual molecules.

On the other hand, scaling should be able to account for systematic matrix shifts. The latter can be caused by nondirectional, isotropic physical effects that do not depend on the shape and symmetry of the cavity. Scaling factors can then statistically account for the matrix shifts even if the physical mechanisms responsible for the shifts are not known.

In Figure 4 experimentally observed differences between the gas-phase and the Ar-matrix frequencies are shown for the 347 fundamental vibrational frequencies in the training set as a function of the experimental gas-phase frequency. There are
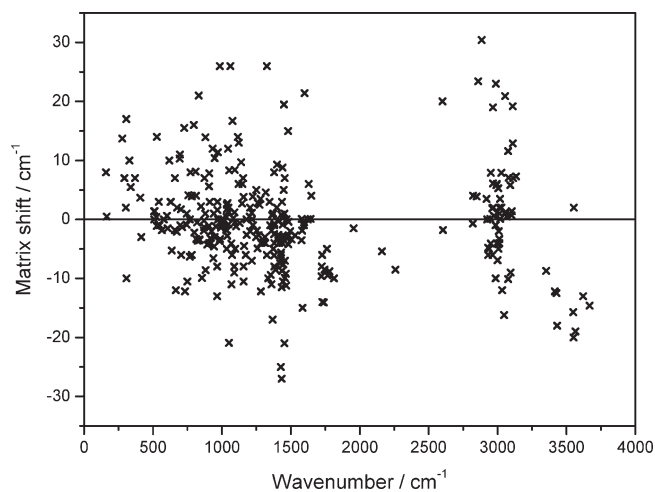
Figure 4. Experimental matrix shifts ($\tilde{\nu}_{Ar,exp} - \tilde{\nu}_{gas,exp}$ vs $\tilde{\nu}_{gas,exp}$) for the vibrational modes of the training set.

regions where, except for a few exceptions, the matrix shifts are systematic. The most conspicuous among these are the N−H and O−H stretching regions at ∼3200−3500 cm^{-1}, where the Ar-matrix data are red-shifted by 10−20 cm^{-1}. The matrix shift of these vibrational modes can be accounted for by using different SQM scaling factors for Ar-matrix and gas-phase spectra.

There are chaotic regions in Figure 4 as well. In the C−H stretching region at ∼2800−3100 cm^{-1} the matrix shifts vary essentially randomly between +10 and −20 cm^{-1}. Although it cannot be seen directly, it is well-known in matrix isolation spectroscopy, including the studies used for the present fits, that C−H stretching modes are frequently split in Ar matrices due to site effects, causing both red- and blue-shifted bands compared to gas-phase observations. Thus, the matrix shifts of the C−H stretching modes are not expected to be reflected in the different gas-phase and Ar-matrix SQM scaling factors.

Finally there are regions, which might seem to be chaotic at first sight, but where tendencies can be shaded. In the fingerprint region, especially around 800−1200 cm^{-1}, different bending and stretching vibrations can strongly mix in the normal modes. If the Ar matrix has a consistent effect on different types of internal coordinates (and on the corresponding force constants), then the standard SQM scaling model ought to be able to handle this situation.

After summarizing our expectations, let us analyze the fitting results. The largest, most pronounced difference between the gas-phase and Ar-matrix scaling factors are observed for the X−X−X−X torsional force constants where the Ar-matrix scaling factors are about 2−3% larger than the corresponding gas-phase scaling factors. This is most likely caused by the fact that these torsions usually have large amplitudes which are hindered in a tight matrix cage.

The Ar-matrix scaling factors for X−{Cl,S} stretches are about 1% smaller than the corresponding gas-phase scaling factors. This can be explained either by the relatively stronger dispersion forces between Ar and Cl/S that weaken the X−{Cl,S} covalent bond, or by coupling of the X−{Cl,S} stretching vibration with Ar lattice vibrations which increase the reduced mass of the vibrational mode.

As expected, there is also a relatively large difference between the gas-phase and Ar-matrix scaling factors for the N−H and

4645

dx.doi.org/10.1021/jp201907y |*J. Phys. Chem. A* 2011, 115, 4640–4649
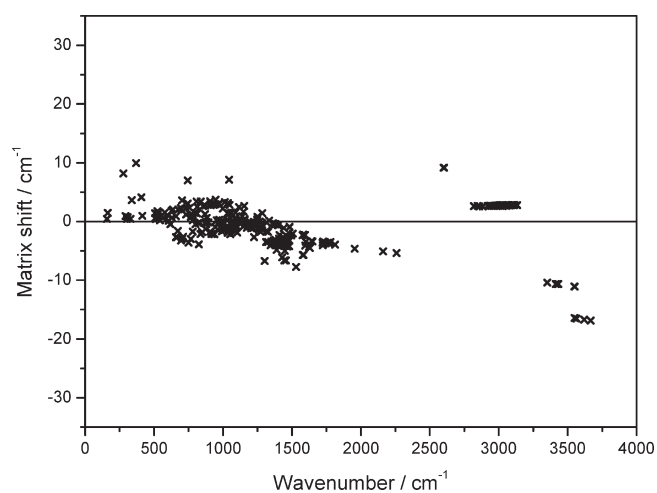
Figure 5. B3LYP/6-31++G** SQM matrix shifts ($\tilde{\nu}_{Ar,SQM} - \tilde{\nu}_{gas,SQM}$ vs $\tilde{\nu}_{gas,exp}$) for the vibrational modes of the training set.

O−H stretching force constants where the Ar-matrix value is smaller by about 0.6% and 0.9%, respectively, than the corresponding gas-phase value. Similar results are obtained for the H−N−H and H−C−H force constants with a decrease larger than 1%. In contrast the S−H stretching force constants are larger by about 0.7% in the Ar matrix than in the gas phase. This might be due to the fact that, unlike the N−H and O−H groups, the S−H group tightly fits into an Ar hole in the matrix which makes the potential energy surface steeper along the S−H stretching coordinate.

It is also in line with expectations that there is no significant difference between the Ar-matrix and gas-phase scaling factors for the C−H stretching force constants. The same holds for the X−X (e.g., C−C) stretch, the X−X−H bend, and the {H,X}−X−X−X torsion scaling factors. In the case of X−X stretching force constants in particular, the practically identical Ar-matrix and gas-phase scaling factors are explained by the fact that most of these internal coordinates are located inside the molecule and are affected by the matrix only indirectly.

As a summary Figure 5 shows the differences between the SQM scaled gas-phase and Ar-matrix frequencies as obtained at the B3LYP/6-31++G** level of theory for the 347 fundamental vibrational frequencies in the training set. It is clear from the above discussion, from Figure 5, as well as from a comparison with Figure 4 that this simple model has the potential of predicting the correct matrix shift even in regions where different vibrational modes overlap and mix. Further examples are provided in the next section.

3.3. Illustrative Tests. The following calculations are included in order to demonstrate the quality of results that can be obtained with the new SQM scaling factors. None of these systems (except the formamide monomer) were included in the training set.

3.3.1. Hydrogen-Bonded Molecular Systems. In order to check the accuracy of the fitted SQM scaling factors for the four functionals we have selected a few hydrogen-bonded test systems: the *Cc* conformer of hydroxyacetone (*Cc* HA), the $t\gamma_L+$ conformer of *N*-acetylproline amide (Ac-Pro-NH$_2$), the β_{DL} and $\gamma_{D=L}$ conformers of *N*-acetylglycine-*N'*-methyl amide (Ac-Gly-NHMe), and the formamide dimer.

The results for systems with intramolecular hydrogen bonds are presented in Tables 3 and 4. All the SQM fits except for PBE show a slight improvement in the total rms error for *Cc* HA (see

Table 3. Absolute Errors (in cm^{-1}) in Calculated $\tilde{\nu}_{O-H}$ and $\tilde{\nu}_{C=O}$ Vibrational Frequencies for the *Cc* Conformer of Hydroxyacetone Together with RMS Errors (also in cm^{-1}) for All Experimentally Available Frequencies^a

method	$\Delta\tilde{\nu}_{O-H}$	$\Delta\tilde{\nu}_{C=O}$	rms^b
uniformly scaled B3LYP/6-31++G**	+49	−13	24.23
SQM B3LYP/6-31G*	+17	+5	11.66
SQM B3LYP/6-31++G**	+8	−6	9.81
SQM B3LYP/aug-cc-pVTZ	+2	−7	9.61
SQM M06-2X/6-31++G**	+23	+12	10.94
SQM M06-2X/aug-cc-pVTZ	+22	+9	9.92
SQM B3PW91/6-31++G**	−12	−7	9.73
SQM B3PW91/aug-cc-pVTZ	−19	−6	11.03
SQM PBE/6-31++G**	−51	−22	16.67
SQM PBE/aug-cc-pVTZ	−58	−31	20.60

^{a} Experimental values are observed in Ar matrix, from ref 41. ^{b} Root-mean-square errors of 6 vibrational frequencies.

Table 3) as compared to the results obtained using the original SQM B3LYP/6-31G* scheme. For the O−H stretching mode directly affected by intramolecular hydrogen bonding, the SQM B3LYP/6-31++G** and the SQM B3LYP/aug-cc-pVTZ results show definitive improvement as compared to SQM B3LYP/6-31G*. In line with the conclusions of Section 3.1, the 6-31++G** and aug-cc-pVTZ basis sets give almost the same result for each functional.

For the amide A (N−H stretching), I (C=O stretching) and II (mixed N−H stretching and C−N−H deformation) modes of the peptide models (see Table 4), which are also directly affected by intramolecular hydrogen bonding, the advantage of the SQM B3LYP/6-31++G** scheme over SQM B3LYP/6-31G* is more noticeable; for the amide A mode the rms error is reduced by almost a factor of 2. In both these cases SQM M06-2X/6-31++G** seems to perform particularly well.

For the formamide dimer, the test system with an intermolecular hydrogen bond, conclusions similar to those above also hold (see Table 5). Both the larger N−H frequency stretching and the C=O stretching modes are estimated rather well with each scheme, while the lower frequency N−H stretching mode has a smaller error when the SQM B3LYP/6-31++G** or the SQM B3LYP/aug-cc-pVTZ schemes are used instead of SQM B3LYP/6-31G*. For this mode, the M06-2X and B3PW91 functionals also perform well. Unlike for the training set and for the test systems with intramolecular hydrogen bonds, the aug-cc-pVTZ basis set gives a considerably better result for this mode of the formamide dimer than the 6-31++G** basis set.

3.3.1. Systems Containing S and Cl Atoms. trans-Thioglyoxal (HCOCHS), chloro-methanol (ClCH$_2$OH), and 3,4-dichloro-1,2,5-thiadiazol (DCTD) were chosen as test systems containing heavier atoms (S and Cl). The rms errors for vibrational frequencies computed using the different functionals, new SQM scaling factors, and the 6-31++G** basis set are compared with older scaling schemes in Table 6. As expected, the SQM procedure gave better results than uniform scaling for the B3LYP functional. The results obtained using the new SQM scaling factors with the 6-31++G** basis set are slightly better than those obtained by the formerly published B3LYP/6-31G* SQM scaling scheme. Note that for these systems the other three functionals perform better than B3LYP. Apart from HCOHCS the best results are obtained using the M06-2X functional. The observation regarding the good

4646

dx.doi.org/10.1021/jp201907y |*J. Phys. Chem. A* 2011, 115, 4640–4649

Table 4. RMS Errors (in cm^{-1}) in Calculated Amide A, Amide I and II Vibrational Frequencies for the $t\gamma_L+$ Conformer of Ac-Pro-NH$_2$ and the β_{DL} and $\gamma_{D=L}$ Conformers of Ac-Gly-NHMe as Well as RMS Errors for All Experimentally Available Frequencies of $t\gamma_L+$ of Ac-Pro-NH$_2$[a]

method	rms[b] amide A	rms[b] amide I	rms[c] amide II	rms[d] Ac-Pro-NH$_2$
uniformly scaled B3LYP/6-31++G**	36.78	20.96	12.62	22.61
SQM B3LYP/6-31G*	19.05	14.64	16.50	10.14
SQM B3LYP/6-31++G**	9.99	10.87	15.88	9.32
SQM M06-2X/6-31++G**	14.91	7.73	14.46	11.43
SQM B3PW91/6-31++G**	19.46	7.44	18.77	9.71
SQM PBE/6-31++G**	40.66	11.87	17.39	17.53

[a] Experimental values are observed in Ar matrix, from refs 42 and 43. [b] Root-mean-square errors of 6 vibrational frequencies. [c] Root-mean-square errors of 4 vibrational frequencies. [d] Root-mean-square errors of 53 vibrational frequencies.

Table 5. Absolute Errors (in cm^{-1}) in Calculated Vibrational Frequencies for the Formamide Dimer[a]

method	$\Delta\tilde{\nu}_{N-H, aa}$	$\Delta\tilde{\nu}_{N-H, as}$	$\Delta\tilde{\nu}_{C=O}$
SQM B3LYP/6-31G*	−2	+55	+8
SQM B3LYP/6-31++G**	0	+42	−11
SQM B3LYP/aug-cc-pVTZ	−12	+14	−17
SQM M06-2X/6-31++G**	−9	+40	−9
SQM M06-2X/aug-cc-pVTZ	−6	+16	−16
SQM B3PW91/6-31++G**	−13	−7	−7
SQM B3PW91/aug-cc-pVTZ	−13	−26	−11
SQM PBE/6-31++G**	−15	−80	−8
SQM PBE/aug-cc-pVTZ	−15	−99	−22

[a] Experimental values are observed in gas phase, from ref 44.

Table 6. RMS Errors (in cm^{-1}) in Calculated Vibrational Frequencies for trans-Thioglyoxal (HCOCHS), Chloromethanol (ClCH$_2$OH), and 3,4-Dichloro-1,2,5-thiadiazol (DCTD)

method	rms[a] HCOCHS	rms[b] ClCH$_2$OH	rms[c] DCDT
uniformly scaled B3LYP/6-31++G**	14.17	43.24	31.81
SQM B3LYP/6-31G*	13.71	18.00	21.61
SQM B3LYP/6-31++G**	11.29	14.19	19.73
SQM M06-2X/6-31++G**	15.42	12.76	11.30
SQM B3PW91/6-31++G**	8.38	13.58	13.53
SQM PBE/6-31++G**	15.47	16.51	17.47

[a] Experimental values are observed in Ar matrix, from ref 45. Root-mean-square errors of 8 vibrational frequencies. [b] Experimental values are observed in gas phase from ref 46. Root-mean-square errors of 6 vibrational frequencies. [c] Experimental values are observed in gas phase, from ref 47. Root-mean-square errors of 13 vibrational frequencies.

Table 7. Experimental and Calculated Ar-Matrix Shifts (in cm^{-1}) for HNO$_3$ and trans-HONO

	HNO$_3$			trans-HONO		
	expt[30,32]	PCM[34]	SQM[a]	expt[31,33]	PCM[35]	SQM[a]
$\Delta\tilde{\nu}_{O-H}$	−28	−79	−16	−20	−71	−17
$\Delta\tilde{\nu}_{N=O}$	−11	−18	−3	−11	−13	−4
	−5	−6	−2			
$\Delta\tilde{\nu}_{H-O-N}$	+1	+5	−1	+2	+1	0
$\Delta\tilde{\nu}_{N-O}$	+18	+2	+1	+8	+6	+1
$\Delta\tilde{\nu}_{O-N-O}$	+1	+2	+2	+13	+8	0
	+9	+7	0			
$\Delta\tilde{\nu}_{torsion}$	+8	+5	+2	+5	+1	+2
	−7	−8	+1			

[a] Present study. Obtained as the difference of SQM B3LYP/6-31++G** calculations using gas-phase and Ar-matrix scaling factors.

3.3.1. Matrix Shift. Since there are no significant differences in matrix shifts obtained by different functionals and/or basis sets, we discuss only comparison of the SQM B3LYP/6-31++G** matrix shifts with experimental data.

The first example includes HNO$_3$ and trans-HONO. Each vibrational mode of both molecules has been observed both in the gas phase[30,31] and in an Ar matrix;[32,33] furthermore, the matrix shifts have previously been estimated using the polarizable continuum model (PCM).[34,35] These former computational and experimental results together with our SQM B3LYP/6-31++G** matrix shifts are collected in Table 7. As can be seen the O−H stretching mode is largely overestimated by the PCM method, while our results show good and almost perfect agreement for HNO$_3$ and trans-HONO, respectively. For N=O stretching frequency shifts the PCM and the SQM results have about the same error, but opposite sign; i.e., the PCM results overestimate, while the SQM results underestimate, the matrix shifts. For lower frequency vibrations the PCM model unambiguously gives better values.

Similarly to HNO$_3$ and trans-HONO, the matrix shift of the O−H stretching mode of glycine is well estimated by the SQM scheme; the estimated shift is −16.5 cm^{-1}, which compares to the experimental value of −17 cm^{-1}.[11a,36] The sign of the shift for the C−O−H bending and C=O stretching vibrations are estimated well by our model, although their magnitudes are underestimated; i.e., the computed shifts are only −2 cm^{-1} and −4 cm^{-1}, respectively, while the corresponding experimental matrix shifts are −13 cm^{-1} and −8 cm^{-1}. For the C−N−H bending mode the

performance of the SQM M06-2X/6-31++G** scheme for these systems is also consistent with the fitting results, viz. the residual rms errors of all experimentally available frequencies of the 9 S- and Cl-atom containing molecules in the training set (using the gas-phase scaling factors obtained for the whole training set) are 13.18 cm^{-1} and 12.74 cm^{-1} for B3LYP/6-31++G** and M06-2X/6-31++G**, respectively.

For frequency calculations for systems containing S and Cl atoms, the SQM M06-2X/6-31++G** scheme seems to be the preferred choice, especially if the molecule has weak X−Cl or X−S bonds, or when dispersion interactions between S or Cl atoms and other fragments of the molecule might be important.

4647

dx.doi.org/10.1021/jp201907y |J. Phys. Chem. A 2011, 115, 4640–4649

estimated and the experimental matrix shifts have opposite signs, -4 cm^{-1} and $+10$ cm^{-1}, respectively.

As a conclusion our simple model for predicting matrix shifts works only for certain types of vibrations, e.g., for O−H stretchings and possibly for low frequency torsional modes. Even so, for interpretation of matrix isolation IR spectra the use of Ar matrix scaling factors is recommended over the gas-phase sets. As an example, using the gas-phase instead of Ar-matrix B3LYP/6-31++G** scaling factors the rms error increases from 9.70 to 13.30 cm^{-1} when the computed frequencies are compared to Ar-matrix experimental values for glycine. For the Ar-matrix vibrational frequencies of the molecules in the fitting set the change from Ar-matrix to gas-phase B3LYP/6-31++G** scaling factors results in a more than 1 cm^{-1} larger rms error for frequencies larger than 2500 cm^{-1} and smaller than 500 cm^{-1}, while the difference in the rms errors is only about 0.5 cm^{-1} in the fingerprint region.

4. SUMMARY

In the present work we have determined quantum mechanical (SQM) scaling factors for four DFT functionals (PBE, B3LYP, B3PW91, and M06-2X) using two different basis sets (6-31++G** and aug-cc-pVTZ). The main aims of the work were (1) to obtain a scheme which yields more accurate computed vibrational frequencies especially for systems with intra- or intermolecular hydrogen bonds; (2) to include S- and Cl-containing molecules in the fitting procedure; (3) to try to estimate the matrix shifts between gas-phase and Ar-matrix isolation vibrational frequencies by using two different sets of SQM scaling factors.

The fitting results and the test calculations revealed that the accuracy obtained using the 6-31++G** and the aug-cc-pVTZ basis sets are approximately the same.

As far as the functionals are concerned, PBE gives the best unscaled frequencies, but the worst scaled frequencies. The opposite is true for the M06-2X functional, which, among the four functionals tested, gives the largest rms errors in the unscaled vibrational frequencies, but when using the SQM scheme its rms error is only slightly larger than that with the B3LYP and B3PW91 functionals. When using the SQM scheme the rms errors decrease by about a factor of 2 as compared to uniformly scaled vibrational frequencies, while the improvement can be as large as a factor of 6 when compared to unscaled frequencies.

For simple molecules containing elements only up to the second row the SQM procedure in conjunction with either the B3LYP or B3PW91 density functionals can be recommended on the basis of our results. For hydrogen-bonded systems the use of the SQM B3LYP procedure, together with either the 6-31++G** or the aug-cc-pVTZ basis set, is suggested. We obtained small but definite improvements, i.e., a 10−30% reduction of the rms error compared to the originally published SQM B3LYP/6-31G* scheme for hydrogen-bonded test systems. For systems containing heavier atoms, e.g., sulfur, the SQM M06-2X scheme seems to be the best choice from among the investigated methods.

As far as the modeling of the matrix shifts is concerned we obtained less satisfactory results. The significantly different gas-phase/Ar-matrix scaling factors for the O−H and N−H stretching and X−X−X−X torsional modes reproduce the matrix shift remarkably well for vibrational modes whose normal coordinates have a high enough component of these internal coordinates.

In order to improve the estimation of matrix shifts by simple scaling, the fact that double and triple bonds usually have a larger polarizability and larger interaction with the matrix than do single bonds has to be taken into account. Furthermore, atoms and bonds inside the molecule do not interact directly with the matrix, unlike those on the surface. Although both of these effects *could* be taken into account, algorithms to treat surface atoms and bonds and/or multiple bonds separately would complicate the present simple scheme. Use of the SQM scheme together with a solvent model might also improve the theoretical estimate of the matrix shifts.

In the near future we intend to determine similar SQM scaling factors for recent functionals, including the DFT-D methods, which account for dispersion interactions.[37−40]

■ ASSOCIATED CONTENT

ⓢ Supporting Information. Experimental gas-phase and Ar-matrix vibrational frequencies of the training set molecules together with the corresponding references. This material is available free of charge via the Internet at http://pubs.acs.org.

■ AUTHOR INFORMATION

Corresponding Author
*E-mail: tarczay@chem.elte.hu.

■ ACKNOWLEDGMENT

■ REFERENCES

(1) (a) Pulay, P.; Fogarasi, G.; Pang, F.; Boggs, J. E. *J. Am. Chem. Soc.* **1979**, *101*, 2550. (b) Fogarasi, G.; Pulay, P. *J. Mol. Struct.* **1986**, *141*, 145.

(2) Biczysko, M.; Panek, P.; Scalmani, G.; Bloino, J.; Barone, V. *J. Chem. Theory Comput.* **2010**, *6*, 2115.

(3) (a) Nielsen, H. H. *Rev. Mod. Phys.* **1951**, *23*, 90. (b) Clabo, D. A., Jr.; Allen, W. D.; Remington, R. B.; Yamaguchi, Y.; Schaefer, H. F., III. *Chem. Phys.* **1988**, *123*, 187. (c) Allen, W. D.; Yamaguchi, Y.; Császár, A. G.; Clabo, D. A., Jr.; Remington, R. B.; Schaefer, H. F., III. *Chem. Phys.* **1990**, *145*, 427. (d) Willetts, A.; Handy, N.; Green, W.; Jayatilaka, D. *J. Phys. Chem.* **1990**, *94*, 5608. (e) Barone, V.; Bloinoa, J.; Guidoa, C. A.; Lipparinia, F. *Chem. Phys. Lett.* **2010**, *496*, 157.

(4) Frisch, M. J.; Trucks, G. W.; Schlegel, H. B.; Scuseria, G. E.; Robb, M. A.; Cheeseman, J. R.; Scalmani, G.; Barone, V.; Mennucci, B.; Petersson, G. A.; Nakatsuji, H.; Caricato, M.; Li, X.; Hratchian, H. P.; Izmaylov, A. F.; Bloino, J.; Zheng, G.; Sonnenberg, J. L.; Hada, M.; Ehara, M.; Toyota, K.; Fukuda, R.; Hasegawa, J.; Ishida, M.; Nakajima, T.; Honda, Y.; Kitao, O.; Nakai, H.; Vreven, T.; Montgomery, J. A., Jr.; Peralta, J. E.; Ogliaro, F.; Bearpark, M.; Heyd, J. J.; Brothers, E.; Kudin, K. N.; Staroverov, V. N.; Kobayashi, R.; Normand, J.; Raghavachari, K.; Rendell, A.; Burant, J. C.; Iyengar, S. S.; Tomasi, J.; Cossi, M.; Rega, N.; Millam, N. J.; Klene, M.; Knox, J. E.; Cross, J. B.; Bakken, V.; Adamo, C.; Jaramillo, J.; Gomperts, R.; Stratmann, R. E.; Yazyev, O.; Austin, A. J.; Cammi, R.; Pomelli, C.; Ochterski, J. W.; Martin, R. L.; Morokuma, K.; Zakrzewski, V. G.; Voth, G. A.; Salvador, P.; Dannenberg, J.J.; Dapprich, S.; Daniels, A. D.; Farkas, Ö.; Foresman, J. B.; Ortiz, J. V.; Cioslowski,

4648

dx.doi.org/10.1021/jp201907y |*J. Phys. Chem. A* 2011, 115, 4640–4649

J.; Fox, D. J.*Gaussian 09, Revision A.1*; Gaussian, Inc.: Wallingford, CT, 2009.

(5) Crawford, T. D.; Sherrill, C. D.; Valeev, E. F.; Fermann, J. T.; King, R. A.; Leininger, M. L.; Brown, S. T.; Janssen, C. L.; Seidl, E. T.; Kenny, J. P.; Allen, W. D. PSI3: An Open-Source Ab Initio Electronic Structure Package. *J. Comput. Chem.* **2007**, *28*, 1610. See http://www.psicode.org.

(6) Lotrich, V.; Flocke, N.; Ponton, M.; Yau, A; Perera, A.; Deumens, E.; Bartlett, R. J. *J. Chem. Phys.* **2008**, *128*, 194104.

(7) CFOUR, a quantum chemical program package written by Stanton, J. F.; Gauss, J.; Harding, M. E.; Szalay, P. G., with contributions from Auer, A. A.; Bartlett, R. J.; Benedikt, U.; Berger, C.; Bernholdt, D. E.; Christiansen, O.; Heckert, M.; Heun, O.; Huber, C.; Jonsson, D.; Jusélius, J.; Klein, K.; Lauderdale, W. J.; Matthews, D.; Metzroth, T.; O'Neill, D. P.; Price, D. R.; Prochnow, E.; Ruud, K.; Schiffmann, F.; Stopkowicz, S.; Tajti, A.; Varner, M. E.; Vázquez, J.; Wang, F.; Watts, J. D., and the integral packages MOLECULE (Almlöf, J.; Taylor, P. R.), PROPS (Taylor, P. R.), ABACUS (Helgaker, T.; Jensen, H. J. Aa.; Jørgensen, P.; Olsen, J.), and ECP routines by Mitin, A. V.; van Wüllen, C., For the current version, see http://www.cfour.de.

(8) Császár, A. G. Anharmonic Molecular Force Fields. In *Encyclopedia of Computational Chemistry*; Wiley: New York, 2002.

(9) Polyansky, O. L.; Császár, A. G.; Shirin, S. V.; Zobov, N. F.; Barletta, P.; Tennyson, J.; Schwenke, D. W.; Knowles, P. J. *Science* **2003**, *299*, 539.

(10) (a) Merrick, J. P.; Moran, D.; Radom, L. *J. Phys. Chem. A* **2007**, *111*, 11683. and citations therein.(b) NIST Computational Chemistry Comparison and Benchmark DataBase, http://http://cccbdb.nist.gov.

(11) See, for example: (a) Linder, R.; Seefeld, K.; Vavra, A.; Kleinermanns, K. *Chem. Phys. Lett.* **2008**, *453*, 1. (b) Kunttu, H.; Dahlqvist, M.; Murto, J.; Räsänen, M. *J. Phys. Chem.* **1988**, *92*, 1495. (c) Gloaguen, E.; Valdes, H.; Pagliarulo, F.; Pollet, R.; Tardivel, B.; Hobza, P.; Piuzzi, F.; Mons, M. *J. Phys. Chem. A* **2010**, *114*, 2973. (d) Tarczay, G.; Zalyubovsky, S. J.; Miller, T. A. *Chem. Phys. Lett.* **2005**, *406*, 81.

(12) Pulay, P.; Fogarasi, G.; Pongor, G.; Boggs, J. E.; Vargha, A. *J. Am. Chem. Soc.* **1983**, *105*, 7037.

(13) Fogarasi, G.; Zhou, X.; Taylor, P. W.; Pulay, P. *J. Am. Chem. Soc.* **1992**, *114*, 8191.

(14) Rauhut, G.; Pulay, P. *J. Phys. Chem.* **1995**, *99*, 3093.

(15) Pulay, P. *J. Mol. Struct.* **1995**, *347*, 293.

(16) Baker, J.; Jarzecki, A. A.; Pulay, P. *J. Phys. Chem. A* **1998**, *102*, 1412.

(17) Kalincsák, F.; Pongor, G. *Spectrochim. Acta, Part A* **2002**, *58*, 999.

(18) Borowski, P.; Drzewiecka, A.; Fernández-Gómez, M.; Fernández-Liencres, M. P.; Ruiz, T. P. *Vib. Spectrosc.* **2010**, *52*, 16.

(19) (a) Hehre, W. J.; Ditchfield, R.; Pople, J. A. *J. Chem. Phys.* **1972**, *56*, 2257. (b) Francl, M. M.; Petro, W. J.; Hehre, W. J.; Binkley, J. S.; Gordon, M. S.; DeFrees, D. J.; Pople, J. A. *J. Chem. Phys.* **1982**, *77*, 3654. (c) Clark, T.; Chandrasekhar, J.; Schleyer, P.v.R. *J. Comput. Chem.* **1983**, *4*, 294. (d) Krishnam, R.; Binkley, J. S.; Seeger, R.; Pople, J. A. *J. Chem. Phys.* **1980**, *72*, 650. (e) Gill, P. M. W.; Johnson, B. G.; Pople, J. A.; Frisch, M. J. *Chem. Phys. Lett.* **1992**, *197*, 499.

(20) (a) Dunning, T. H., Jr. *J. Chem. Phys.* **1989**, *90*, 1007. (b) Woon, D. E.; Dunning, T. H., Jr. *J. Chem. Phys.* **1994**, *100*, 2975. (c) Dunning, T. H., Jr. *J. Chem. Phys.* **1989**, *90*, 1007. (d) Kendall, R. A.; Dunning, T. H., Jr.; Harrison, R. J. *J. Chem. Phys.* **1992**, *96*, 6796. (e) Woon, D. E.; Dunning, T. H. J. *Chem. Phys.* **1993**, *98*, 1358.

(21) Riley, K. E.; Holt, B. T. O.; Merz, K. M., Jr. *J. Chem. Theory Comput.* **2002**, *3*, 407.

(22) Zhao, Y.; Truhlar, D. G. *J. Phys. Chem. A* **2005**, *109*, 5656.

(23) (a) Becke, A. D. *J. Chem. Phys.* **1993**, *98*, 5648. (b) Lee, C.; Yang, W.; Parr, R. G. *Phys. Rev. B* **1988**, *37*, 785.

(24) (a) Perdew, J. P.; Burke, K.; Ernzerhof, M. *Phys. Rev. Lett.* **1996**, *77*, 3865. (b) Perdew, J. P.; Burke, K.; Ernzerhof, M. *Phys. Rev. Lett.* **1997**, *78*, 1396.

(25) (a) Zhao, Y.; Truhlar, D. G. *Theor. Chem. Acc.* **2008**, *120*, 215. (b) Zhao, Y.; Truhlar, D. G. *Acc. Chem. Res.* **2008**, *41*, 157.

(26) (a) Perdew, J. P.; Chevary, J. A.; Vosko, S. H.; Jackson, K. A.; Pederson, M. R.; Singh, D. J.; Fiolhais, C. *Phys. Rev. B* **1992**, *46*, 6671.E: 1993, *48*, 4978. (b) Perdew, J. P.; Burke, K.; Wang, Y. *Phys. Rev. B* **1996**, *54*, 16533.E: 1998, *57*, 14999.

(27) Magyarfalvi, G.; Tarczay, G.; Vass, E. *Wiley Interdisciplinary Reviews: Computational Molecular Science* **2011**, *1*, 403.

(28) *PQS version 3.2*; Parallel Quantum Solutions: Fayetteville, AR.

(29) Puzzarini, C.; Biczysko, M.; Barone, V. *J. Chem. Theory Comput.* **2010**, *6*, 828.

(30) (a) McGraw, G. E.; Bernitt, D. L.; Hisatsune, I. C. *J. Chem. Phys.* **1965**, *42*, 237. (b) Bair, C. H.; Brockman, P. *Appl. Opt.* **1979**, *18*, 4152. (c) Maki, A. G.; Wells, J. S. *J. Mol. Spectrosc.* **1980**, *82*, 427. (d) May, R. D.; Webster, C. R.; Molina, L. T. *J. Quant. Spectrosc. Radiat. Transfer* **1987**, *38*, 381. (e) Tan, T. L.; Looi, E. C.; Lua, K. T. *J. Mol. Spectrosc.* **1992**, *155*, 420. (f) Perrin, A.; Flaud, J.-M.; Camy-Peyret, C.; Jaouen, V.; Farrenq, R.; Guelachvili, G.;; *J. Mol. Spectrosc.* **1993**, *160*, 524. (g) Harwood, M. H.; Jones, R. L.; Cox, R. A.; Lutman, E.; Rattigan, O. V. *J. Photochem. Photobiol., A* **1993**, *73*, 167. (h) Tan, T. L.; Wang, W. F.; Looi, E. C.; Ong, P. P. *Spectrochim. Acta* **1996**, *52A*, 1315.

(31) (a) Guilmot, J.-M.; Godefroid, M.; Herman, M. *J. Mol. Spectrosc.* **1993**, *160*, 387. (b) Deeley, C. M.; Mills, I. M.; Halonen, L. O.; Kauppinen, J. *Can. J. Phys.* **1985**, *63*, 962.

(32) (a) Barnes, A. J.; Lasson, E.; Nielsen, C. J. *J. Mol. Struct.* **1994**, *322*, 165. (b) Cheng, B.-M.; Lee, J.-W.; Lee, Y.-P. *J. Phys. Chem.* **1991**, *95*, 2814. (c) Chen, W.-J.; Lo, W.-J.; Cheng, B.-M.; Lee, Y.-P. *J. Chem. Phys.* **1992**, *97*, 7167.

(33) (a) Talik, T.; Tokhadze, K. G.; Mielke, Z. *Phys. Chem. Chem. Phys.* **2000**, *2*, 3957. (b) Mielke, Z.; Talik, T.; Tokhadze, K. G. *J. Mol. Struct.* **1999**, *484*, 207. (c) Mielke, Z.; Latajka, Z.; Kolodziej, J.; Tokhadze, K. G. *J. Phys. Chem.* **1996**, *100*, 11610. (d) Mielke, Z.; Tokhadze, K. G.; Latajka, Z.; Ratajczak, E. *J. Phys. Chem.* **1996**, *100*, 539.

(34) Liu, G.; Zhang, X. *THEOCHEM* **2007**, *807*, 179.

(35) Liu, G.; He, T. *THEOCHEM* **2007**, *817*, 55.

(36) Stepanian, S. G.; Reva, I. D.; Radchenko, E. D.; Rosado, M. T. S.; Duarte, M. L. T. S.; Fausto, R.; Adamowicz, L. *J. Phys. Chem. A* **1998**, *102*, 1041.

(37) Chai, J.-D.; Head-Gordon, M. *Phys. Chem. Chem. Phys.* **2008**, *10*, 6615.

(38) Thanthiriwatte, K. S.; Hohenstein, E. G.; Burns, L. A.; Sherrill, C. D. *J. Chem. Theory Comput.* **2011**, *7*, 88.

(39) Riley, K. E.; Pitonak, M.; Jurecka, P.; Hobza, P. *Chem. Rev.* **2010**, *110*, 5023.

(40) Zhang, I. Y.; Xu, X. *Int. Rev. Phys. Chem.* **2011**, *30*, 115.

(41) Sharma, A.; Reva, I.; Fausto, R. *J. Phys. Chem. A* **2008**, *112*, 5935.

(42) Pohl, G.; Perczel, A.; Vass, E.; Magyarfalvi, G.; Tarczay, G. *Phys. Chem. Chem. Phys.* **2007**, *9*, 4698.

(43) Pohl, G.; Perczel, A.; Vass, E.; Magyarfalvi, G.; Tarczay, G. *Tetrahedron* **2008**, *64*, 2126.

(44) Albrecht, M.; Rice, C. A.; Suhm, M. A. *J. Phys. Chem. A* **2008**, *112*, 7530.

(45) Torres, M.; Clement, A.; Strausz, O. P. *Nouv. J. Chim.* **1983**, *7*, 269.

(46) Wallington, T. J.; Schneider, W. F.; Barnes, I.; Becker, K. H.; Sehested, J.; Nielsen, O. J. *Chem. Phys. Lett.* **2000**, *322*, 97.

(47) Pasinszki, T.; Tarczay, G. Unpublished results.

4649

dx.doi.org/10.1021/jp201907y |*J. Phys. Chem. A* 2011, 115, 4640–4649